



Density functional study of diamond epitaxy on the (111) and (100) surfaces of copper

V.G. Zavodinsky

Institute for Materials Science, the Russian Academy of Sciences 153 Tikhooskanskaya, 680042, Khabarovsk, Russia

Received 27 April 2005; received in revised form 28 April 2005; accepted 29 April 2005

Available online 24 May 2006

Abstract

Ab initio calculations show that epitaxial diamond films can be grown on copper substrates with geometry parameters close to those of bulk diamond. The mean cohesive energy for C(100) films are larger than that for C(111) films; however the C(111) films are more stable than the C(100) ones with respect to separation from the copper substrate. The latter fact explains why the preferable observed orientation of diamond microcrystallites on copper is the $\langle 111 \rangle$ one.

© 2005 Elsevier B.V. All rights reserved.

Keywords: Diamond film; Simulation; Heteroepitaxy

1. Introduction

Thin diamond films have been grown on non-diamond substrates by a number of techniques. The non-diamond substrates can be classified into two main categories: (1) carbide forming materials and (2) materials which have no affinity for carbon. Copper seems a promising candidate to be a substrate material for epitaxy growth of diamond films. First, its lattice parameter (3.608 Å) is similar to that of diamond (3.567 Å). Second, it has no carbon affinity. Therefore, there is a set of experimental works on this subject [1–9]. The main result of these studies is that diamond crystallites grown on polycrystalline copper can mount up to the 20-micrometer thickness with the preferable orientation of $\langle 111 \rangle$. However, as far as I know, there are no theoretical supports for such experimental studies. The present work is devoted to study the first stages of diamond epitaxy on copper in the framework of the density functional theory.

2. Method and details of calculations

The calculations were performed using the FHI96md simulation code [10] based on the density functional theory, pseudopotential method, and the plane wave basis set. The generalized gradient approximation in the Perdew and Wang form (PW91) [11] for the exchange and correlation functional and fully separable Troullier–Martins pseudopotentials [12] were employed. The pseudopotentials were constructed using the FHI98pp code [13]; they were verified to avoid ghost states and to describe the basic experimental characteristics of the bulk materials. The d component of the pseudopotential for carbon and the s component for copper were adopted as local ones. I used the (0.25;0.25;0.00) point for the k -space integrations for slabs, whereas the Gamma point was applied for bulk Cu–C calculations; the energy cut-off of 40 Ry was applied in all calculations. Test calculations have been executed with use of nine points. Geometry parameters (bond distances and bond–bond angles) were found to be very similar to those for the one-point case (mismatches are of about 1%). Energy parameters differed from one-point values by 0.1–0.3 eV and kept the general laws inherent in the one-point calculations.

E-mail address: vzavod@mail.ru.

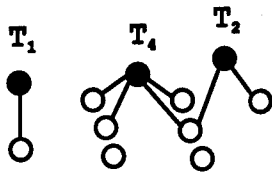


Fig. 1. Positions for a single carbon atom on the Cu(100) surface. White circles are surface copper atoms, black circles are carbon atoms.

The carbon pseudopotential was tested for diamond. The equilibrium lattice constant a_0 and bulk modulus B_0 , calculated using Murnaghan equation of state [14], are equal to 3.57 Å and 450 GPa, respectively. They agree well with the experimental values equal to 3.567 Å and 443 GPa [15]. The pseudopotential for Cu was verified for the *fcc* bulk copper with the number of k -points of 40. I calculated the lattice constant to be 3.64 Å and the bulk modulus to be 142 GPa. The experimental reference values are 3.61 Å and 138 GPa [16].

The (111) and (100) surfaces of Cu were represented by five-layers slabs with the 2×2 surface unit cell separated by a 20 Å thick vacuum space, and only the first surface layer atoms of Cu were relaxed. To avoid the artificial electrostatic dipole field, which arises from the asymmetry of the slab, I used a dipole correction [17].

In order to compare the energetic preferences of different carbon phases and carbon–copper systems I calculated the mean cohesive energy per carbon atom, $E_{\text{coh}}(\text{mean})$:

$$E_{\text{coh}}(\text{mean}) = E(C_a) - \frac{E(\text{Cu} - \text{C}) - E(\text{slab})}{N_C}$$

where $E(\text{Cu} - \text{C})$ is the energy of the Cu–C system consisting of the Cu slab and N_C atoms of carbon; $E(\text{slab})$ is the energy of the Cu slab, $E(C_a)$ is the energy of an isolated C atom. For comparison I have calculated cohesive energies for bulk graphite and diamond: they are 8.74 eV and 8.55 eV, respectively. These values overestimate experimental data (7.37 eV for graphite and 7.35 eV for diamond [18]). This is a usual overestimation of the DFT LDA and GGA calculations for carbon materials [19–22]. The calculated C–C bond distances are 1.43 Å for graphite and 1.55 Å for diamond compared with the experimental values of 1.42 Å and 1.53 Å, respectively. The equilibrium graphite inter-planar distance has been found to be 8.65 Å. This value is much larger than the experimental one (6.708 Å). However, it is a typical GGA overestimation: see for instance Ref. [23]) where the value of 8.946 Å has been reported.

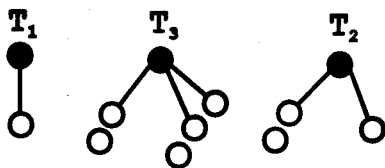


Fig. 2. Positions of a single carbon atom on the Cu(111) surface. White circles are surface copper atoms, black circles are carbon atoms.

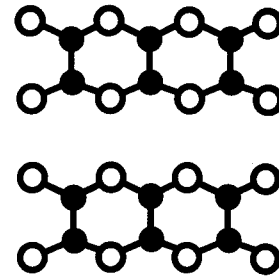


Fig. 3. A dimerized carbon monolayer on the Cu(100) surface. White circles are surface copper atoms, black circles are carbon atoms.

The mean cohesive energy $E_{\text{coh}}(\text{mean})$ includes deposits from internal, surface and interface carbon atoms. Obviously, the internal bonds must be more similar to the bulk bonds than others. In order to compare the C–C bonding in the internal atomic layers of the epitaxial films with that of bulk diamond, I have calculated the internal cohesive energy $E_{\text{coh}}(\text{internal})$ as a function of the number of monoatomic layers L using the following expression:

$$E_{\text{coh}}(\text{internal}) = \frac{E(\text{Cu} - \text{C})_{L-2} - E(\text{Cu} - \text{C})_L + 2 \times N_C(\text{layer}) \times E_C}{2 \times N_C(\text{layer})}$$

where the $N_C(\text{layer})$ is the number of carbon atoms in a monoatomic layer. L increases from 4 to 12 for the (100) film and from 5 to 13 for the (111) film with a step of 2. The step of 2 was chosen to keep surface carbon atoms at the same geometry conditions.

3. Results and discussion

3.1. Single carbon atoms on copper surfaces

To study adsorption of single carbon atoms on the Cu(100) surface I placed them in different positions (Fig. 1): (T_1) just above the surface Cu atoms; (T_2) in bridge sites, between two surface Cu atoms; (T_4) above the center of a square formed by four surface Cu atoms. Calculations have shown that the T_1 and T_4 sites are not stable. Being placed in them a carbon atom moves spontaneously to the T_2 site with the equilibrium C–Cu distance $d(\text{C} - \text{Cu})$ of 1.83 Å and the binding energy E_{coh} of 8.67 eV. Thus, the binding energy

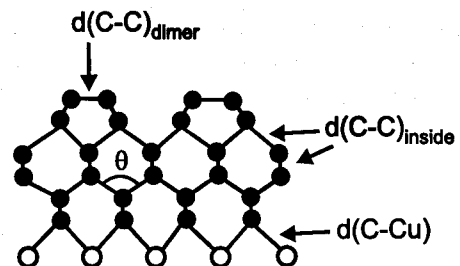


Fig. 4. An atomic scheme of the epitaxial diamond film on the Cu(100) surface.

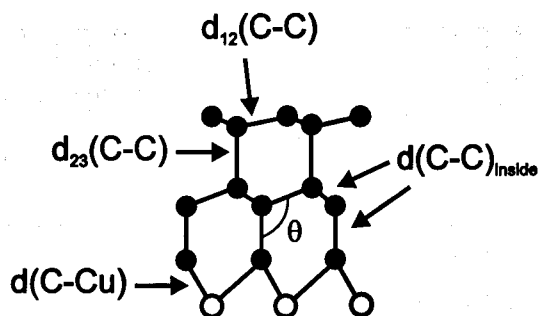


Fig. 5. Atomic scheme of the epitaxial diamond film on the Cu(111) surface.

for a single C atom on the Cu(100) surface is practically the same as that for graphite.

Adsorption of carbon on the Cu(111) surface (Fig. 2) was studied placing C atoms in T_1 (on-top), T_2 (bridge) and T_3 (above the center of a surface atomic triangle) positions. C atoms have moved from the T_1 and T_2 positions to the T_3 position without any barrier. The T_3 position has been found to be the most favorable one with $E_{\text{coh}}=5.82$ eV and $d(\text{C}-\text{Cu})=1.90$ Å.

3.2. Carbon monolayers on copper surfaces

Carbon monolayers on the Cu(100) surface were constructed in two ways: (1) C atoms were placed in T_1 (on-top) positions; (2) C atoms were positioned in T_2 sites. In both cases C atoms left the initial positions and formed C–C dimers situated between two pairs of surface Cu atoms as it is shown in Fig. 3. The dimer length is 1.27 Å, and the Cu–C bond lengths are equal to 1.96 Å. The cohesive energy E_{coh} is equal to 7.07 eV.

In the Cu(111) case I have studied two initial configurations: (1) C atoms are positioned in the “on-top” sites; (2) C atoms are placed in the T_3 -sites. Calculations have shown that the “on-top” carbon monolayers are not stable on the Cu(111) surface. Being placed 1.80 Å above the surface Cu atoms, C atoms have moved up and formed straight atomic chains with an inside C–C distance $d(\text{C}-\text{C})=1.30$ Å. These chains are situated 2.79 Å above the copper surface and have the carbon cohesive energy of 7.65 eV.

Another situation has been found for the case where carbon atoms were placed in the T_3 positions. This C monolayer is stable with the C–Cu distance $d(\text{C}-\text{Cu})$ of 2.01 Å and the cohesive energy E_{coh} of 4.32 eV. In

Table 1
Geometry parameters for the C(100)/Cu(100) epitaxial system

The number of carbon atomic layers, L	2	4	6	8	10	12
$d(\text{C}-\text{Cu})$, Å	1.90	1.95	1.95	1.94	1.94	1.94
$d(\text{C}-\text{C})_{\text{inside}}$, Å	—	1.56	1.58	1.57	1.56	1.56
$d(\text{C}-\text{C})_{\text{dimers}}$, Å	1.41	1.40	1.39	1.38	1.38	1.38
θ , degree	—	122.0	112.3	110.1	109.8	109.7

Table 2
Geometry parameters for the C(111)/Cu(111) epitaxial system

The number of carbon atomic layers, L	3	5	7	9	11	13
$d(\text{C}-\text{Cu})$, Å	1.94	1.97	1.95	1.94	1.94	1.94
$d(\text{C}-\text{C})_{\text{inside}}$, Å	—	1.57	1.56	1.56	1.55	1.55
$d(\text{C}-\text{C})_{12}$, Å	1.50	1.50	1.50	1.51	1.51	1.50
$d(\text{C}-\text{C})_{23}$, Å	1.55	1.72	1.71	1.70	1.70	1.70
θ , degree	104.2	109.6	109.4	110.2	109.9	109.6

comparison with the above case this system can be named quasi stable because its total energy is higher. However, it does not destroy itself spontaneously; some energy barrier is needed for it to be destroyed. Thus we can regard this carbon monolayer as a first stage of the diamond epitaxy growth on the Cu(111) surface.

3.3. Epitaxial diamond layers

To study the geometry and energetic features of the diamond epitaxial growth on copper surfaces I constructed L -monolayers diamond films (L was varied from 2 up to 13) contacted with the Cu(100) and Cu(111) surfaces, respectively (see Figs. 4 and 5). In the (111) case the atoms of the bottom C layer were placed in the T_3 positions, whereas in the (100) case they were positioned in the T_2 sites.

It has been found that in the both cases the epitaxial films kept their diamond-like atomic geometry with the tetrahedral bonding. Their surface reconstructions and relaxations are similar to those of free diamond surfaces. Namely, the surface of the (100) film is dimerized. The dimer length is 1.38–1.41 Å, similar to 1.37 Å obtained for the bulk diamond (100)— 2×1 surface by the LDA [24] and quasi-particle [25] calculations. For the (111) relaxed surface I have obtained the surface C–C distance $d(\text{C}-\text{C})_{12}$ of 1.50–1.51 Å and the undersurface C–C distance $d(\text{C}-\text{C})_{23}$ of 1.50–1.51 Å, close to values of 1.46 Å and 1.68 Å, reported by Kern et al. [24] for the bulk diamond (111) surface.

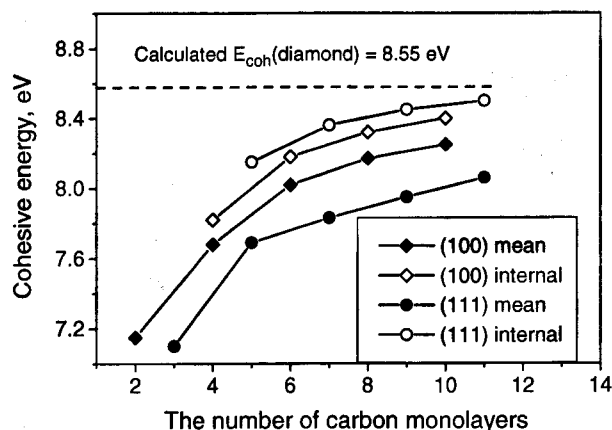


Fig. 6. The cohesive energy (mean and internal) for C(100) and C(111) epitaxial films as a function of the number of carbon monolayers.

Detail data on the calculated interatomic distances and tetragonal angles δ are collected in Tables 1 and 2.

As it follows from Tables 1 and 2, the geometry parameters for epitaxial diamond films are in satisfactory accordance with those for bulk diamond (especially for the (111) case).

Calculated values of the cohesive energy, $E_{\text{coh}}(\text{mean})$ and $E_{\text{coh}}(\text{internal})$ for C(100) and C(111) epitaxial films formed on the Cu(100) and Cu(111) surfaces are plotted in Fig. 6. One can see that $E_{\text{coh}}(\text{internal})$ fits the calculated cohesive energy for diamond (8.55 eV) rather better than $E_{\text{coh}}(\text{mean})$.

To study the stability of the film-substrate bonding I have calculated the film-substrate adhesion energy E_{adh} :

$$E_{\text{adh}} = \frac{E(\text{Cu} - \text{C}) - [E(\text{slab})_{\text{frozen}} + E(\text{film})_{\text{frozen}}]}{N_{\text{C}}(\text{interface})},$$

where $N_{\text{C}}(\text{interface})$ is the number of the interface carbon atoms. Energies of the separated Cu slab, ($E(\text{slab})_{\text{frozen}}$), and C film ($E(\text{film})_{\text{frozen}}$), have been calculated for the same atomic geometries as they were found for the corresponding carbon/copper systems.

The E_{adh} values characterize the bonding between the carbon film and the copper substrate when they are contacted. However, if we want to study the energetics of the film-substrate separation we need to take into account the relaxation of the carbon film and the copper slab after their separation. The energy difference (per interface atom) between the epitaxial carbon-copper system and the relaxed separated carbon film and the relaxed copper slab can be named the separation energy E_{sep} :

$$E_{\text{sep}} = \frac{E(\text{Cu} - \text{C}) - [E(\text{slab})_{\text{relaxed}} + E(\text{film})_{\text{relaxed}}]}{N_{\text{C}}(\text{interface})}.$$

It should be noted that positive values of E_{sep} correspond to the energetic advantage for the separation of the epitaxial diamond film from the copper substrate.

Dependencies of E_{adh} and E_{sep} on the number of carbon monolayers are plotted in Fig. 7 for both the C(100)/Cu(100) and C(111)/Cu(111) systems. One can see that the energy of the bonding of the diamond epitaxial film with the copper substrate (E_{adh}) increases (in the absolute value) with the increase of film thickness and aspires to the value of -2.55 eV for the C(100) films and -2.0 eV for the C(111) films. However, the stability of the film-substrate systems characterized by E_{sep} is not so simple a thing. Fig. 7 demonstrates that the diamond layers thicker than 8 ML are not stable on the Cu(100) substrate ($E_{\text{sep}} > 0$). In other words, the thick diamond films cannot grow on the Cu(100) surface. On another hand, the films formed on the Cu(111) surface have a tendency to be stable when their thickness becomes larger than 9 monolayers ($E_{\text{sep}} < 0$). These results correlate with experimental data [8–10]

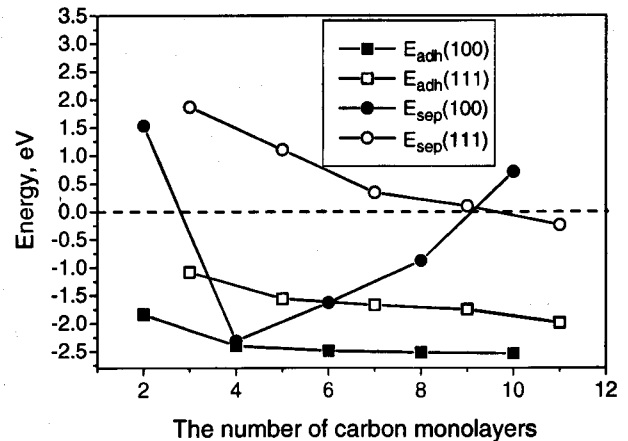


Fig. 7. Adhesion and separation energies for epitaxial diamond films formed on Cu(100) and Cu(111) substrates.

showing that diamond microcrystallites grown on the copper polycrystalline substrates have the (111) orientation mainly.

4. Summary

Ab initio calculations show that epitaxial diamond films can be grown on copper substrates with geometry parameters similar to those of bulk diamond. The mean cohesive energy for the C(100) films are larger than that for the C(111) films; however, the C(111) films are more stable against the separation from the copper substrate. The latter fact explains why the preferable observed orientation of diamond microcrystallites on copper is the $\langle 111 \rangle$ one.

This work has been supported by the Fundamental Research Program of the Russian Academy of Sciences ("Fundamental problems of physics and chemistry for nanosized systems and nanomaterials", 2004), and by the Ministry of Education of the Russian Federation (the grant # 16-11, 2003–2004) and the Russian Foundation of Basic Research (the grant # 06-02-96000, 2006–2007).

References

- [1] M.L. Hartsell, L.S. Plano, J. Mater. Res. 9 (1994) 921.
- [2] J. Narayan, V.P. Godbole, G. Matera, R.K. Singh, J. Appl. Phys. 71 (1992) 966.
- [3] T.P. Ong, F. Xiong, R.P.H. Chang, C.W. White, J. Mater. Res. 7 (1992) 2429.
- [4] R. Ramesham, F.M. Rose, A. Allerman, Diamond Relat. Mater. 1 (1992) 907.
- [5] S.I. Ojika, S. Yamashita, K. Kataoka, T. Ishikara, Jpn. J. Appl. Phys. 32 (Part 2) (1993) L1681.
- [6] S.D. Wolter, B.R. Stoner, J.T. Glass, Diamond Relat. Mater. 3 (1994) 1188.
- [7] Q.H. Fan, J. Gracio, E. Pereira, Diamond Relat. Mater. 6 (1997) 422.
- [8] M. Sommer, R. Haubner, B. Lux, Diamond Relat. Mater. 9 (2000) 351.
- [9] N. Ali, Q.H. Fan, W. Ahmed, I.U. Hassan, C.A. Rego, I.P. O'Hare, Thin Solid Films 355–356 (1999) 162.

- [10] M. Bockstedte, A. Kley, J. Neugebauer, M. Scheffler, *Comp. Phys. Commun.* 107 (1997) 187.
- [11] J.P. Perdew, Y. Wang, *Phys. Rev.*, B 33 (1986) 8800;
J.P. Perdew, J.A. Chevary, S.H. Vosko, K.A. Jackson, M.R. Pederson, D.J. Singh, C. Fiolhais, *Phys. Rev.*, B 46 (1992) 6671.
- [12] N. Troullier, J.L. Martins, *Phys. Rev.*, B 43 (1991) 1993.
- [13] M. Fuchs, M. Scheffler, *Comp. Phys. Commun.* 119 (1999) 67.
- [14] F.D. Murnaghan, *Proc. Natl. Acad. Sci. U. S. A.* 30 (1944) 244.
- [15] I.V. Aleksandrov, A.F. Goncharov, A.N. Zisman, S.M. Stishov, *Sov. Phys. JETP* 66 (1987) 384.
- [16] C.J. Smithells, *Metals Reference Book*, 4th ed., Butterworths, London, 1967, p. 708.
- [17] J. Neugebauer, M. Scheffler, *Phys. Rev.* 46 (1992) 16067.
- [18] R. Weast (Ed.), *CRC Handbook of Chemistry and Physics*, 65th edition, CRC Press Inc., Boca Raton, 1984–1985, p. d58.
- [19] H.J.F. Jansen, A.F. Freeman, *Phys. Rev.*, B 35 (1987) 8207.
- [20] L.H. Li, J.E. Lowther, *J. Phys. Chem. Solids* 58 (1997) 1607.
- [21] B. Farid, R.J. Needs, *Phys. Rev.*, B 45 (1992) 1067.
- [22] J. Chelikowsky, S.G. Lonic, *Phys. Rev.*, B 29 (1984) 3470.
- [23] A. Incze, A. Pasturel, C. Chatillon, *Surf. Sci.* 537 (2003) 55.
- [24] G. Kern, G.J. Hafner, J. Futhmüller, G. Kresse, *Surf. Sci.* 352–354 (1996) 745.
- [25] C. Kress, M. Fiedler, V.G. Schmidt, F. Bechstedt, *Surf. Sci.* 331–333 (1995) 1152.